



HHS Public Access

Author manuscript

Nat Struct Mol Biol. Author manuscript; available in PMC 2015 August 01.

Published in final edited form as:

Nat Struct Mol Biol. 2015 February ; 22(2): 116–123. doi:10.1038/nsmb.2955.

K63 polyubiquitination is a new modulator of the oxidative stress response

Gustavo M. Silva¹, Daniel Finley², and Christine Vogel¹

¹Center for Genomics and Systems Biology, New York University, New York, New York, USA

²Department of Cell Biology, Harvard Medical School, Boston, Massachusetts, USA

Abstract

Ubiquitination is a post-translational modification that signals multiple processes, including protein degradation, trafficking, and DNA repair. Polyubiquitin accumulates globally during the oxidative stress response, which has been mainly attributed to increased ubiquitin conjugation and perturbations in protein degradation. Here we show that the unconventional K63-linked polyubiquitin accumulates in the yeast *Saccharomyces cerevisiae* subjected to peroxides in a highly sensitive and regulated manner. We demonstrated that hydrogen peroxide inhibits the deubiquitinating enzyme Ubp2 leading to accumulation of K63 conjugates assembled by the Rad6-Bre1 ubiquitin conjugase and ligase, respectively. Using linkage-specific isolation methods and SILAC-based quantitative proteomics, we identified >100 new K63 polyubiquitinated targets, which were significantly enriched in ribosomal proteins. Finally, we demonstrated that impairment of K63 ubiquitination during oxidative stress impacts polysome stability and protein expression, rendering cells more sensitive to stress, revealing a new redox-regulatory role for this modification.

INTRODUCTION

Oxidative stress is a frequent challenge to cellular homeostasis, and can be triggered by a variety of endogenous and environmental factors^{1,2}. The molecular damage generated by oxidants impairs cellular viability while promoting carcinogenesis, and is an underlying cause of many human diseases, particularly those of the nervous system^{3–5}. To avoid the harmful consequences of oxidative stress, eukaryotic cells have evolved numerous counteracting mechanisms including the regulation of translation, protein degradation, and

Reprints and permissions information is available at www.nature.com/reprints/index.html.

Corresponding authors: Gustavo M. Silva (gustavo@nyu.edu) and Christine Vogel (cvogel@nyu.edu).

AUTHOR CONTRIBUTIONS

G.M.S. conceived the project. All authors designed the experiments and G.M.S. conducted the experiments. G.M.S. and C.V. wrote the manuscript. All authors discussed the results and commented on the manuscript.

COMPETING FINANCIAL INTERESTS

The authors declare no competing financial interests.

ACCESSION CODES

The mass spectrometry proteomics data have been deposited to the ProteomeXchange Consortium (<http://proteomecentral.proteomexchange.org>) via the PRIDE partner repository with the dataset identifiers PXD000960 and PXD000979.

Any Supplementary Information and Source Data files are available in the online version of the paper.

expression of protective antioxidant genes⁶. Protein ubiquitination is an important feature of the oxidative stress response, known to direct unneeded, damaged, and potentially toxic proteins to the proteasome for degradation⁷.

Ubiquitination is a post-translational modification catalyzed by an enzymatic cascade that comprises a ubiquitin activating enzyme (E1), a ubiquitin conjugating enzyme (E2), and a ubiquitin ligase (E3)⁸. The selectivity of the reaction depends on the E2-E3 pair, which is able to recognize, interact, and conjugate ubiquitin to specific protein substrates. In addition, deubiquitinating enzymes (DUBs) are responsible for controlling the levels of protein ubiquitination by reversing the modification^{9,10}. The yeast genome encodes one E1, eleven E2s, 60-100 E3s, and 20 DUBs¹¹. Since each E2-E3 pair and the corresponding DUBs regulate a specific set of targets in a specific biological process, their identification is essential to understanding the regulatory role of ubiquitination.

Conjugation of polyubiquitin chain to a target protein has initially been characterized as a signal for protein degradation¹², which still appears to be a dominant role. However, polyubiquitination can trigger multiple functions, depending on which lysine residue (K) in the ubiquitin sequence is used to extend the polyubiquitin chain¹³⁻¹⁵. K48 polyubiquitin is the most abundant linkage type in the yeast *S. cerevisiae* (~29 %) and the major signal for protein degradation. K11 and K63 linkages are also abundant (~28 % and ~16 %, respectively)¹⁶. While K11 also serves as a signal for protein degradation, e.g. during the regulation of cell cycle and the endoplasmic reticulum associated protein degradation^{16,17}, K63 ubiquitin fulfills other roles such as endocytosis by the endosomal and vacuolar sorting complexes^{18,19}, DNA damage response²⁰, and activation of the nuclear factor- κ B and T-cell receptor pathways in mammalian cells^{21,22}. In contrast to the well-studied K48 linkage type, much less is known about the regulation and roles of K63 ubiquitination; only a handful of targets have been characterized in yeast¹¹.

Cellular exposure to oxidants induces global ubiquitination^{23,24}, which is thought to trigger degradation of oxidized proteins by the proteasome. This view has been challenged as evidence for ubiquitin-independent degradation of oxidized proteins arose^{25,26}; therefore, the role of increased ubiquitination under stress remains elusive. Moreover, little is known about the targets of the different ubiquitin linkage types, the specific ubiquitinating-deubiquitinating enzymes catalyzing the reactions, and the dynamics of the ubiquitin linkages during the stress response.

To understand the role of protein ubiquitination under oxidative stress, we combined a new linkage-specific ubiquitin isolation tool, quantitative proteomics, and targeted genetic approaches. We observed a rapid and strong pulse of K63 ubiquitin in yeast treated with hydrogen peroxide (H₂O₂), impacting translation and the overall stress response. We also identified the enzymatic sensors that specifically trigger K63 ubiquitination in response to peroxides – representing a new aspect of a fundamental signaling pathway. Our findings represent the first large-scale analysis for a linkage specific ubiquitination under a very common stress suggesting that a concerted and highly regulated ubiquitination response is crucial to determine the cellular fate.

RESULTS

K63 ubiquitin rapidly accumulates during oxidative stress

We set out to characterize the role of polyubiquitination during the oxidative stress response, and monitored the dynamics of the three most abundant ubiquitin linkages (K11, K48 and K63) in a wild-type yeast strain expressing a single ubiquitin gene (WT - SUB280). While both K48 and K63 ubiquitin responded strongly and rapidly to H_2O_2 treatment (Fig. 1a and Supplementary Fig. 1a, b), K11 response was very weak and seemed limited to few targets (Supplementary Fig. 1c). K48 levels sustained over four hours in the recovery medium, but K63 polyubiquitination rose and declined rapidly, falling below detection levels immediately during the recovery phase in fresh medium (Fig. 1a) or after 90 min of prolonged incubation with H_2O_2 (Fig. 1b). This strong pulse of K63 ubiquitination during the oxidative stress response has not been reported before.

We verified the results by targeted mass spectrometry, which we used to quantify the relative abundances of K48 and K63 polyubiquitin linkages via signature peptides obtained from tryptic digest^{27,28}. The mass spectrometry data confirmed that both K48 and K63 linkages increase in response to stress, but K63 ubiquitination increases more strongly and decreases more rapidly than K48 ubiquitination (Fig. 1c and Supplementary Fig. 1d–g). Less abundant ubiquitin linkages (K6, K27, K29 and K33) may also be important for cell response to stress, however, the remainder of this study focuses on delineation of the roles and regulation of this so-far unknown K63-ubiquitination linked signaling pathway.

Next, we investigated the specificity of the K63 ubiquitination response to oxidative stress by testing other environmental stresses. While K48 ubiquitination responded to a wide array of toxic treatments, such as 1.5 mM diamide, heat shock at 37 °C, and salt stress (1 M NaCl), most likely to remove damaged and unnecessary proteins, K63 ubiquitination reacted exclusively to H_2O_2 and other peroxides (Fig. 1d, e). Both organic and inorganic peroxides triggered the accumulation of K63 ubiquitin conjugates, while cells treated with paraquat, an anion radical superoxide generator, were unaffected (Fig. 1e).

We found that the K63 response occurred quickly and across a wide range of H_2O_2 concentrations (Supplementary Fig. 1h, i). We chose an H_2O_2 concentration of 0.6 mM for further experiments since it induced accumulation of K63 ubiquitin without compromising cellular viability (Supplementary Fig. 1j, k). We also showed that the K63 ubiquitin response to peroxides may be conserved in mammalian cells: K63 conjugates accumulated after H_2O_2 treatment in mouse neuronal HT22 cells (Supplementary Fig. 1l). The exact mechanism of the mammalian K63 response remains to be investigated.

K63 ubiquitination is regulated by Rad6, Bre1, and Ubp2

Accumulation of ubiquitinated targets depends on the interplay between conjugation mediated by ubiquitinating enzymes and the reverse reaction catalyzed either by deubiquitinating enzymes or by proteasomal or autophagic degradation of the targets. Degradation of polyubiquitinated targets can either replenish the pool of free ubiquitin by the action of associated DUBs, or under some circumstances, also digest the ubiquitin

molecules. Both, the inhibition of deubiquitinating enzymes or inhibition of the proteasome can lead to accumulation of polyubiquitinated conjugates²⁹.

We conducted a number of targeted tests to identify the specific E2-E3 ubiquitin enzyme pair responsible for conjugation of K63 ubiquitin chains. To do so, we screened a collection of deletion mutants in non-essential E2 enzymes for defects in H₂O₂-induced K63 conjugation. Only one mutant, *rad6* Δ , substantially and highly specifically decreased K63 polyubiquitination in response to H₂O₂ (Fig. 2a). Rad6 is a multi-functional protein known to interact with three different E3s to perform different functions (Supplementary Fig. 2a). These functions include regulation of the cell cycle checkpoint and transcription (Rad6-Bre1)³⁰⁻³², degradation of proteins (Rad6-Ubr1)^{33,34}, and DNA repair (Rad6-Rad18)²⁰. When we tested these three known interaction partners, only the *bre1* Δ strain was defective in promoting K63 ubiquitination under stress, which implied Bre1 to be the E3 partner for Rad6-dependent K63 polyubiquitination in our experiments (Fig. 2b).

Next, we showed that Rad6-Bre1 mediated K63 ubiquitination in response to H₂O₂ is completely independent from the enzymes' previously known functions and targets, suggesting a new redox signaling pathway. First, deletion of the Rad6-Bre1 cofactors, which are essential for activation of the histone H2B monoubiquitination signaling cascade^{30,35-38}, did not hamper the cellular ability to accumulate K63 conjugates (Supplementary Fig. 2b). In addition, the H2B K123R mutated strain, which is incapable of monoubiquitinating histone H2B, still accumulated K63 ubiquitin in response to oxidative stress (Supplementary Fig. 2c). Second, we showed that the accumulation of K63 polyubiquitin under oxidative stress is also independent of Rad6's known role in post-replicative DNA repair through monoubiquitination of PCNA²⁰. As H₂O₂ treatment could induce DNA damage and therefore indirectly trigger the PCNA-linked pathway, we tested for K63 ubiquitination in response to a DNA-damaging reagent. When cells were treated with methyl methanesulfonate (MMS), which methylates DNA, stalls the replication fork, and causes DNA double strand breaks³⁹, K63 conjugates did not accumulate (Supplementary Fig. 2d).

Finally, we demonstrated that K63 ubiquitin response to stress does not depend on the cells arresting in the G2-M phase. Previous work showed that K63 ubiquitination of a single ribosomal protein Rpl28 depends on the phase of the cell division cycle and is most prominent during the G2-M phase⁴⁰. When treating an asynchronous culture of WT_{col} yeast cells for 45 min with H₂O₂, cells did not arrest in G2-M (Supplementary Fig. 2e).

Next, we tested if accumulation of K63 ubiquitinated proteins was linked to increased transcription or translation. Given that the induction of K63 ubiquitin is very rapid (within < 5 min of H₂O₂ treatment - Supplementary Fig. 1h), regulation at the transcription or translation level was very unlikely. Indeed, inhibition of these processes by actinomycin-D or cycloheximide, respectively, did not change the K63 ubiquitin response to H₂O₂ (Supplementary Fig. 2f, g).

We also showed that accumulation of K63 conjugates is independent of protein degradation. It has been shown that K63 ubiquitination targets proteins for degradation^{41,42}, however, inhibition of the proteasome by MG-132 led to accumulation of K48 conjugates but did not

alter the balance of K63 ubiquitin (Supplementary Fig. 2h). Moreover, neither inhibition of autophagy by 3-methyl adenine (3-MA) nor by deletion of *ATG7* gene, essential for the autophagy pathway, increased the accumulation of K63 targets under stress (Supplementary Fig. 2i, j).

In sum, we showed that the increase of K63-linked polyubiquitin in response to peroxides was independent of transcription, translation, DNA damage, protein degradation, or other known roles and targets of the Rad6-Bre1 enzyme pair. Therefore, we investigated the role of DUBs in the rapid accumulation of K63 ubiquitin in response to H₂O₂, specifically through inhibition of their activity during stress. First, we showed that cellular incubation with PR-619, a broad spectrum DUB inhibitor, led to accumulation of both K63 and K48 conjugates (Supplementary Fig. 3a). Further, we measured the global *in vitro* activity of DUBs after cellular treatment with H₂O₂ using the fluorescent substrate Ub-AMC. DUBs activity towards Ub-AMC was promptly inhibited by H₂O₂ treatment and reversed by *in vitro* incubation with the reducing agent dithiothreitol (DTT) (Fig. 3a) – providing first lines of evidence for the role of DUB inhibition in the K63 ubiquitination pathway.

Next, we narrowed the group of potential deubiquitinating enzymes to the class of cysteine DUBs. In yeast, DUBs are grouped into two classes depending on their active site. The UBP (USP in humans), the OTU and the UCH families are marked by the dependence on a reactive cysteine in the enzyme's catalytic center; while Rpn11, the single JAMM-MPN+ member in yeast, is a metalloprotease coordinating zinc ions in its catalytic site⁹⁻¹¹. We showed that *in vitro* reversal of endogenous K63 conjugates strongly and specifically depends on reactive cysteines. K63 ubiquitin was readily reversed by DTT and completely inhibited by iodoacetamide (IAM), a thiol reducing agent and a thiol alkylator, respectively (Supplementary Fig. 3b). In contrast, treatment with EDTA, a metal chelator, had no effect on K63 removal. To identify the specific DUB responsible for regulating K63 ubiquitination during oxidative stress, we screened a collection of null mutants in cysteine DUBs for a phenotype of K63 accumulation. The *ubp2Δ* strain showed a high level of K63 ubiquitin in the absence of oxidative stress (Fig. 3b and Supplementary Fig. 3c) and even after two hours of prolonged exposure to H₂O₂, confirming that Ubp2 is controlling K63 homeostasis during the oxidative stress response (Fig. 3c and Supplementary Fig. 3d).

Further, we characterized Ubp2's activity towards removal of K63 polyubiquitin and its sensitivity to H₂O₂ using the purified enzyme and several *in vitro* approaches. We showed that Ubp2 activity against fluorogenic Ub-AMC or K63 tetra-polyubiquitin chains was reversibly inhibited by H₂O₂ (Fig. 3d, e and Supplementary Fig. 3e). Moreover, Ubp2 was able to remove K63 polyubiquitin from endogenous substrates, which was largely prevented by the presence of H₂O₂ (Fig. 3f). While other DUBs may also remove K63 polyubiquitin chains, albeit more slowly, our results suggest that Ubp2 plays a major role in the accumulation of K63 targets in a mechanism involving acute inhibition of its activity by H₂O₂.

Ribosomes are a main target of K63 ubiquitination

To further characterize the cellular role of K63 polyubiquitin during the oxidative stress response, we identified the K63-ubiquitinated targets by quantitative proteomics. To-date,

no proteomics method was available to analyze targets of a specific ubiquitin linkage type. We developed a new approach in which we used the K63-TUBE isolation system (LifeSensors) to enrich for K63 linkages (Supplementary Fig. 4a), and subjected the proteins to LC-MS/MS analysis. To eliminate contaminants, validate true K63 conjugates, and reduce experimental biases, we performed a stable isotope labeling (SILAC)-based mass spectrometry experiment which paired the WT with the ubiquitin K63R strain (SUB413) after H₂O₂ treatment (Fig. 4a - see Methods and Supplementary Notes for details). The K63R strain expresses a ubiquitin mutant with lysine 63 substituted by arginine, which specifically prevents K63-chain formation (Fig. 1a). In this setup, we identified 115 potential K63 targets in two replicate experiments (Supplementary Table 1), as defined by an at least 50 % increase in abundance relative to the K63R negative control at a 5 % FDR (Supplementary Fig. 4b). In addition, in Supplementary Table 2 we described a core dataset of even higher confidence, reporting 52 K63-ubiquitinated targets identified by two independent search engines (MaxQuant and Proteome Discoverer).

We found that a significant fraction of the K63 targets in the main dataset is involved in translation (GO enrichment at FDR < 0.00002 %), and contains mostly ribosomal proteins and translation elongation factors (Fig. 4b and Supplementary Table 1). The concentration of K63 conjugates spanned over several orders of magnitude indicating that the enrichment in ribosomal proteins is not due to a bias towards high-abundance proteins (Supplementary Fig. 4c), as is often found in mass spectrometry experiments. When mapped to the 3D structure of the ribosome complex, many proteins were located near the aminoacyl-peptidyl binding sites or the exit tunnel (Fig. 4c and Supplementary Fig. 4d).

Next, we showed that ribosomal K63 ubiquitination under oxidative stress appears to help stabilizing the complete 80S complex and the formation of polysomes. When we monitored polysome levels by sucrose sedimentation profiling at physiological ionic strength (3 mM MgCl₂), the K63R mutant displayed strongly increased peaks of the unassembled 40S and 60S subunits (Fig. 5). H₂O₂ is known to reduce the levels of polysomes⁴³, however the K63R mutant subjected to H₂O₂ almost completely lacked polysomes, compared to the wild-type strain with largely intact polysomes (Fig. 5a,b). This phenotype was partially rescued at high-ionic strength which inhibits ribonucleases and stabilizes polysomes (30 mM MgCl₂, Supplementary Fig. 5a). Using this setup, we further validated ribosomal K63 ubiquitination in two different background strains (Figure 5c-e). The majority of K63 labels was distributed across both the monosomal and polysomal fractions in a WT yeast strain exposed to H₂O₂ (Fig. 5c), and, expectedly, no meaningful K63 ubiquitin labeling was detected in the K63R strain treated with H₂O₂ (Fig. 5d). However, the K63R mutant strain still displayed K48 ubiquitin in the polysomal fraction (Supplementary Fig. 5c). Importantly, *rad6Δ* and *bre1Δ* strains did not show detectable levels of K63 ubiquitination in polysomes after H₂O₂ treatment (Fig. 5e), corroborating the role of Rad6-Bre1 in mediating K63 polyubiquitination of ribosomal proteins in response to oxidative stress.

Further, we found that K63 ubiquitination may be a new factor promoting translation during oxidative stress through polysome stabilization, and that K63 levels are affected by perturbation of translation regulatory mechanisms. For example, *GCN2* encodes the kinase that inhibits translation in response to oxidative stress by phosphorylating the alpha subunit

of the eukaryotic translation initiation factor 2^(ref. 2324). We found that the $\Delta gcn2$ strain presents a high level of basal K63 ubiquitination, which is further enhanced in the presence of H₂O₂ (Fig. 6a). Moreover, cellular treatment with 5 μ g/ml puromycin, a translation inhibitor which prematurely terminates protein synthesis by releasing ribosomes, increased the amount of K63 ubiquitin under stress (Fig. 6b). In comparison, the addition of 0.2 μ g/ml rapamycin, which prevents translation initiation, and 200 μ g/ml cycloheximide, which locks the ribosomes onto the mRNA and halts elongation, did not lead to increased K63 ubiquitin under stress (Fig. 6b). Our results also showed that K63 ubiquitin accumulates in cells grown to stationary phase even in the absence of exogenous H₂O₂, a physiological model of oxidative stress where translation is also inhibited (Fig. 6c). Interestingly, the levels of K63 ubiquitin under H₂O₂ treatment were much higher in cells grown to stationary phase than in cells grown to log phase.

Next, we investigated whether K63 polyubiquitination is important for cellular resistance to oxidative stress. In cells deficient of K63 ubiquitination, high levels of H₂O₂ (4 mM) increased the amount of oxidized, and therefore, damaged proteins compared to the wild-type (Fig. 7a). This condition also triggered high levels of K48 ubiquitinated proteins which presumably were *en route* to proteasomal degradation. At 0.6 mM H₂O₂, which is the concentration used throughout our study, the K63R and WT strains accumulated similar amounts of oxidized proteins (Supplementary Fig. 6a). These results suggest that, consistent with impaired translation as indicated by dissociated polysomes and higher levels of oxidative damage, K63R cells are more sensitive to stress than wild-type cells (Fig. 7b).

Similarly, we found that K63 modification impacts the presence and abundance of stress-protective and translation regulatory proteins. Since K63R strain was more sensitive to H₂O₂ than the WT, we investigated by mass spectrometry how the lack of K63 ubiquitin changes protein abundances. Proteomics analysis of the whole cell lysate showed that 133 proteins were down-regulated in the K63R mutant strain when compared to WT upon stress (Fig. 7c, Supplementary Fig. 6b, and Supplementary Table 3), including many stress-related proteins. Proteins involved in ncRNA processing and ribosome biogenesis were significantly enriched amongst the down-regulated genes (FDR < 5 %), consistent with a possible role of K63 ubiquitin in translation regulation.

DISCUSSION

We described a new role for K63-linked polyubiquitination during the cellular response to oxidative stress induced by peroxides. Peroxides such as H₂O₂ are commonly produced by cellular metabolism or by exogenous sources, and represent one of the most common types of reactive oxygen species regulating signaling processes and promoting oxidative stress. We showed that in yeast treated with H₂O₂, K63 ubiquitin spiked immediately and diminished during the recovery phase, while K48 ubiquitination was sustained throughout the experiment. The different dynamics of the ubiquitin linkage types indicate a complex regulatory response managing cellular resistance to a common environmental stress.

Using a combination of new molecular tools, genetics, and systems approaches, we identified the three enzymes, Rad6 (E2 conjugase), Bre1 (E3 ligase) and Ubp2 (DUB) that

Author Manuscript

Author Manuscript

Author Manuscript

Author Manuscript

together define the specific pathway of K63 modification. To the best of our knowledge, this is the first time this function has been highlighted for Rad6-Bre1; the only other yeast E2 enzyme known to produce K63 chains is Ubc13, mediating DNA repair²⁰. Furthermore, we showed that it is the inhibition of Ubp2 which results in the rapid increase of K63 ubiquitin upon peroxide treatment, rather than an increase in ubiquitin conjugation. While it is known that members of the USP family of mammalian DUBs are generally inhibited by H₂O₂ treatment^{45,46}, we demonstrated for the first time that this is also the case in yeast. DUB inhibition through oxidative stress has been proposed *in vitro* and shown for monoubiquitination of PCNA⁴⁵, but its importance during K63 ubiquitination under oxidative stress was previously unknown. Further, some authors have suggested that Ubp2 may function in K63 deubiquitination^{16,47}, but did not envisage its role during oxidative stress. Our results unify these disparate observations: K63 ubiquitin increases in response to oxidative stress through oxidative inhibition of the Ubp2 deubiquitinating enzyme. The specificity of Ubp2 towards K63 polyubiquitin chain is still elusive, and its hydrolase activity against other chain conformations, particularly linear polyubiquitin chains⁴⁸, will be subject to ongoing studies.

Although peroxides can oxidize cysteine residues and inactivate enzymes, not every catalytic cysteine is sensitive to oxidation⁴⁹. Notably, the ubiquitinating enzymes Rad6 and Bre1 also have catalytic cysteines, but appear to be robust towards H₂O₂: even at high peroxide concentrations, cells still accumulated K63 polyubiquitin. Further, if DUBs were inhibited or deleted, yeast cells accumulated K63 ubiquitin even in the absence of H₂O₂. These results suggest a mechanism by which Rad6-Bre1 activity is constitutive, and inactivation of the deubiquitinating enzyme is responsible for the stress-specific ubiquitination. Deletion of any of these three enzymes, Rad6, Bre1, or Ubp2, severely impacts the balance of cellular K63 ubiquitin. Interestingly, it has been recently shown that members of USP family of DUBs (Ubp in yeast) have lower target specificity to distinct ubiquitin linkages than other DUB families⁵⁰, and therefore we hypothesize that Ubp2 - and possibly also the multifunctional Rad6 and Bre1 enzymes - require additional co-factors to achieve target specificity *in vivo*.

This study provides the first large-scale proteomics analysis of a specific ubiquitin linkage type, using a new isolation system and mass spectrometry. We expanded the number of known K63 ubiquitinated targets from a handful^{14,15,51} to over one hundred. These new targets include proteins such as subunits of the V-ATPase VMA complex, cellular permeases, proteins from the Golgi mannosyltransferase complex, and most notably a substantial number of ribosomal proteins (Supplementary Table 1).

The observation of oxidant-regulated ribosome ubiquitination led us to investigate the role of K63 ubiquitin in translation regulation. Our results suggest that K63 ubiquitination in response to oxidative stress serves to stabilize the ribosome complex and polysomes, therefore promoting protein synthesis and cellular viability. While previous studies have identified ubiquitin modifications on ribosomal proteins and even the specific lysine residues on protein targets^{40,52}, the enzymatic digest during sample preparation precluded identification of the ubiquitin linkage type, preventing specific interpretations such as presented here. Only one ribosomal subunit, Rpl28, is known to be K63-ubiquitinated during

cell cycle progression⁴⁰, but without a connection to oxidative stress or the ubiquitinating enzymes that catalyze the reaction.

Our combined results suggest that K63 polyubiquitination stabilizes polysomes during the translation cycle. During every round of mRNA translation, K63 ubiquitin may be conjugated and deconjugated to assist ribosome function (Fig. 7d). This hypothesis is supported by several lines of evidence. First, when DUBs are inhibited by H₂O₂ but translation is still active - as is the case in the $\Delta gcn2$ strain - cells accumulate very high levels of K63 ubiquitin indicating that continuous translation involves K63 ubiquitin. Second, treatment with puromycin, which leads to polysome dissociation due to early translation termination, robustly increases K63 ubiquitin levels. In comparison, cycloheximide and rapamycin, which block translation earlier in the cycle, do not trigger an increased K63 response, indicating that ubiquitination may take place at a later translation step. Third, during the stationary phase, which is known to inhibit translation almost completely and to produce endogenous oxidants⁵³, K63 ubiquitination is highly impacted by the presence of exogenous H₂O₂ and even more so than in cells grown to log phase. Finally, mapping K63-modified proteins to the ribosomal 3D structure suggests that modified subunits may preferentially occur around the ribosome's exit tunnel and therefore impact elongation or termination. In support of this interpretation, work in bacteria has shown that cyclic stabilization of ribosomes is essential in supporting cellular survival and stress tolerance^{54,55}. In eukaryotes, K63 ubiquitination is known to act as a scaffold to assemble protein complexes in several signaling pathways^{14,15,51}. Based on these reports, we hypothesize that K63 ubiquitination could serve to recruit additional factors to enhance stability of the ribosomes-mRNA complex during translation elongation or termination. Validation of this hypothesis and a combined investigation of ribosome structure, modification, and activity in response to stress will be the subject of future work. For example, diglycine lysine antibodies⁵⁶ can be used to identify the exact sites of modification which in turn will provide further insights into the specific role of K63 ubiquitin in ribosome function.

Cells subjected to oxidative stress down-regulate translation globally, but must activate expression of some genes to cope with the oxidative challenge. The abundance of stress-related proteins in yeast appears to be mostly set by transcription, however, increasing evidence suggests key roles of post-transcriptional regulation, in particular at the level of translation^{44,57,58}. Our results indicate that K63 ubiquitination supports expression of antioxidant proteins and therefore cellular stress resistance. We showed that inability to produce K63 polyubiquitin chains in the K63R mutant severely impacts cellular survival and down-regulates a number of important stress-response proteins, such as chaperones Hsp10, Hsp82, Hsc82, and the antioxidant enzymes Trx1, Prx1, Grx2 and Grx5 (Supplementary Table 3).

Collectively, our results demonstrated a new and important regulatory role for K63 polyubiquitination during the oxidative stress response. The Ubp2-dependent accumulation of K63 polyubiquitin supports previous suggestions of cysteine DUBs as sensitive redox biosensors⁴⁶ whose inactivation enables a very rapid response that is independent of transcription, translation, or modification of proteins. Therefore, K63 ubiquitination can

potentially serve as a redox biomarker in yeast and other organisms. Our findings raise many additional questions that will be addressed by future work - for example, how Rad6-Bre1 recognize and ubiquitinate their targets, how ribosomes may be stabilized by ubiquitination, and how higher eukaryotes, such as mammals, use this regulatory pathway. Ubiquitination emerges as a key player during the oxidative stress response by linking traditionally opposing processes in protein expression: the translation machinery responsible for synthesis of proteins and the proteasome system involved in their degradation.

ONLINE METHODS

Cell strains and culture

All yeast *Saccharomyces cerevisiae* strains used in this study are described in the Supplementary Table 4. Standard recombination methods were used to delete genes; deletions were confirmed by PCR. Cells were cultivated at 30 °C in synthetic dextrose minimal medium (SD - 0.67% yeast nitrogen base, 2% dextrose and required amino acids) at 200 rpm agitation. Unless stated otherwise, cells underwent at least 6 divisions and were treated with 0.6 mM H₂O₂ for 45 min in log phase (OD₆₀₀ ~ 0.3 – 0.5). Prior to proteasome inhibition with MG-132, the RJD1171 strain was incubated in minimal proline dextrose medium to induce permeability⁶⁰. Quantitative SILAC experiments were performed in cells grown in SD medium containing the amino acid dropout mixture depleted in arginine and lysine (Sunrise Science Products). SILAC media were supplemented with light or heavy isotopes of arginine and lysine (L-Arg6 ¹³C; L-Lys8 ¹³C, ¹⁵N – Cambridge Isotopes). For serial dilution assay, yeast culture was normalized to OD₆₀₀ of 0.2 after the 45 min pulse of H₂O₂ and sequentially diluted at a 1:5 ratio before spotting onto YPD rich medium plates without H₂O₂. Viability assay was performed using 5 µM FUN1 Cell Stain dye (Life Technologies) according to the manufacturer's protocol. The wild-type strain (WT) used for the majority of the assays was the SUB280 strain. The SILAC experiment used the wild-type GMS280 and the GMS413 K63R ubiquitin mutant strain. The experiments involving the deletion collection (E2-E3 and other null mutants) used a different wild-type herein named WT_{col} (S288c). The DUB deletion experiments used WT_{DUBs} (SUB62). Cell treatment reagents: 3-methyl adenine, actinomycin-D, *t*-butyl hydroperoxide, cumene hydroperoxide, cycloheximide, diamide, H₂O₂, methyl methanesulfonate, paraquat, and puromycin (Sigma), MG-132 (SantaCruz Biotechnologies), PR-619 (LifeSensors) and rapamycin (EMD Millipore).

Mammalian cell culture

The HT22 murine hippocampal cells were cultured in Dulbecco's Modified Eagle's Medium containing 10 % fetal bovine serum and antibiotics (penicillin and streptomycin). Cells were treated for indicated times with 25 μ M H₂O₂ at 70 % confluence. The HT22 cells were a kind gift from Dr. Raj Ratan (Burke Medical Research Institute). Protein extraction was performed by cell sonication in NP40 lysis buffer (50 mM Tris-HCl pH 7.5, 150 mM NaCl, 0.5 % NP40, 20 mM iodoacetamide, 1x EMD Millipore protease inhibitor cocktail set I) prior to western blotting.

Protein preparation

Cells were disrupted by glass-bead agitation at 4 °C in standard buffer: 50 mM Tris-HCl pH 7.5, 150 mM NaCl, 20 mM iodoacetamide (IAM), 1x EMD Millipore protease inhibitor cocktail set I. The extract was cleared by centrifugation and protein concentration was determined by Bradford assay (BioRad). *Protein oxidation* - Oxidized (carbonylated) proteins were derivatized with 2 mM DNPH (2,4-dinitrophenylhydrazine) for 30 min in the presence of 6 % SDS and protected from light. The reaction was neutralized with 1 M Tris, 15 % glycerol and 10 % β -mercaptoethanol prior to western blotting analysis. *Isolation of K63 ubiquitinated proteins* - K63 ubiquitinated proteins were isolated from cell lysate using FLAG K63-TUBE (K63-Tandem Ubiquitin Binding Entities – LifeSensors, cat# UM604) according to manufacturer's protocol. For the pulldown assay, the standard lysis buffer also contained 50 nM of the K63-TUBE peptide and 5 mM EDTA. The cell lysate was incubated for one additional hour at 4 °C after clearing by centrifugation. K63 proteins were immunoprecipitated using magnetic Dynabeads Protein G (Invitrogen) loaded with 7 μ g/mg beads of anti-FLAG antibody (Sigma). The immunoprecipitation was performed for 1 h at 4°C under agitation. K63 targets were eluted with 0.2 M glycine pH 2.5 for 1 h at 4°C. The pH of the eluate was neutralized and trypsin digestion for proteomic analysis was performed as described below. Alternatively, the Dynabeads were boiled in Laemmli buffer containing 10 mM DTT for western blot. Uncropped images of gels and blots used in this study can be found in Supplementary Data Set 1.

Western blotting

Proteins were separated by standard 10% SDS-polyacrylamide gel electrophoresis (SDS-PAGE) loaded in Laemmli buffer containing 10 mM DTT. Samples were transferred to PVDF membrane and immunoblotting was performed using the following antibodies: anti-K63 ubiquitin (1:4,000 - cat# 05-1308, clone apu3, EMD Millipore), anti-K11 ubiquitin (1:1,000 - cat# MABS107, clone 2A3/2E6 EMD Millipore), anti-K48 (1:10,000 - cat# 4289, clone D9D5 - Cell Signaling), anti-actin (1:5,000 - cat# 4967 - Cell Signaling), anti-GAPDH (1:4,000 - cat# ab9485, Abcam), anti-DNP (1:8,000 - cat# D9656 - Sigma). Anti-mouse and anti-rabbit secondary antibodies conjugated with HRP and ECL prime detection reagents were acquired from GE Healthcare Life Sciences. All antibodies have been validated by the manufacturer or are expected to react with the species used in this study based on sequence similarity.

Ubp2 purification and DUB activity

TAP-tagged Ubp2 was purified from 3–5 mg of yeast cell extract (log phase in SD-medium) using magnetic beads conjugated with mouse IgG (Cell Signaling). Beads were washed five times with buffer containing 50 mM Tris-HCl pH 7.5, 150 mM NaCl, and 5 mM EDTA. When specified, purified protein or cell lysate was incubated with 0.5 mM H₂O₂, 10 mM DTT, or 10 mM IAM for 10 to 15 min prior to activity measurement. Activity assays were performed with DUBs attached to the beads or by using 5 μ g of the whole cell lysate. DUB activity was determined at 30 °C using 0.75 μ M Ub-AMC fluorogenic substrate (LifeSensors) and fluorescence kinetics was monitored at 460 nm (exc. at 380 nm). Ubp2

activity against 1 µg K63 tetra-ubiquitin chain (LifeSensors) was monitored *in vitro* by 20 % SDS-PAGE analysis.

Mass spectrometry analysis

Protein preparation for proteomics analysis was performed as previously described⁵⁸. In brief, tryptically digested proteins were separated on a 15 cm Agilent ZORBAX 300 StableBond C18 column (75 µm ID, 3.5 µm particle, 300 Å pore size) by reverse-phase chromatography with a gradient of 5 to 60 % acetonitrile over 3 to 5h, performed with an Eksigent NanoLC 2DPlus liquid chromatography system. The eluted peptides were injected in-line onto an LTQ Orbitrap Velos mass spectrometer (Thermo Scientific). Data-dependent analysis was performed at a resolution of 60,000 and with the top 20 most intense ions selected from each MS full scan, with dynamic exclusion set to 90 s if *m/z* acquisition was repeated within a 45 s interval. To increase coverage and improve quantification, each biological replicate was analyzed 3 to 4 times (technical replicates). The RAW data files were combined and processed using MaxQuant (v. 1.3.0.5 – www.maxquant.org) to identify and quantify protein abundance. The spectra were matched against the yeast *Saccharomyces cerevisiae* database (Uniprot - 2012 release). Protein identification was performed using 10 ppm tolerance at the MS level (FT- mass analyzer) and 0.5 Da at the MS/MS level (Ion Trap analyzer), with a posterior global false discovery rate of 1% based on the reverse sequence of the yeast FASTA file. Up to two missed trypsin cleavages were allowed, oxidation of methionine and N-terminal acetylation were searched as variable post-translational modification, and cysteine carbamidomethylation as fixed. The minimum number of SILAC peptide pairs used for quantitation was set to two. For identification and quantification of K63 ubiquitin targets, only proteins present in both biological replicates containing at least two peptides were considered for further analysis. For an even higher confidence identification of K63 ubiquitinated proteins, the mass spectrometry data were also analyzed with Proteome Discoverer (Thermo Scientific) with matching parameters. Proteins identified by both search engines are listed in Supplementary Table 2. *Targeted mass spectrometry* – Quantitative mass spectrometry measurements of signature peptides of ubiquitin linkages were performed as previously described²⁸ with a few modifications. Briefly, tryptic lysate from SILAC samples was loaded into a 50 cm Easy Spray PepMap C18 column (75 µm ID, 2 µm particle, 100 Å pore size) in-line with a Q-Exactive (Thermo Scientific) mass spectrometer using a 120 min gradient (0 – 40 % ACN). Parallel reaction monitoring²⁷ was performed with a targeted MS2 method using the inclusion list provided in Supplementary Table 5. MS2 data was acquired with a resolution of 17,500, automatic gain control of 5e4, maximum ion time of 250 ms, isolation window of 2 *m/z*, and normalized collision energy of 27. Peptide selection and quantitation was performed after manual inspection using Skyline (MacCoss lab, proteome.gs.washington.edu/software/skyline/). Two biological replicates and two technical injections were averaged for each data point. Gene Ontology analysis (GO) was performed using the DAVID functional annotation tool (<http://david.abcc.ncifcrf.gov/>). Function annotation was performed to assess significance of function enrichment against the background of the proteome identified by mass spectrometry. Sample size was a function of experimental depth (and not a choice of the experimenter). All data were normally distributed or transformed (e.g. by taking the log) to

fit a normal distribution. Variation across replicates is specified whenever replicate experiments are reported.

Polysome analysis

Polysome profiling was performed as described previously⁶¹. Briefly, cells were incubated in the presence of 150 µg/ml cycloheximide for 10 min at 30 °C and lysed immediately in extraction buffer (20 mM Tris-Acetate pH 7.0, 50 mM NaCl, 3 – 30 mM MgCl₂, 20 mM iodoacetamide, 200 µg/ml heparin, 200 µg/ml cycloheximide, 1X cOmplete mini EDTA-free Roche protease inhibitor cocktail). A total of 400 µg of RNA was sedimented by ultracentrifugation for 150 min at 36,000 × rpm (Beckman SW40 rotor) at 4 °C in a 7 to 47 % sucrose gradient (buffered in 50 mM Tris-Acetate pH 7.0, 30 mM MgCl₂, and 200 µg/ml cycloheximide). During sucrose gradient analysis, absorbance was monitored at 254 nm while ~900 µl-fractions were collected using a Brandel density gradient fractionation system. Proteins from polysome fractions were precipitated with TCA-Acetone prior to western blotting.

Flow cytometry analysis

For DNA content analysis, yeast cells were fixed in 70% ethanol overnight. Cells were centrifuged and incubated with 40 µg/ml RNase A in Na-Citrate buffer for 2 h at 50 °C, followed by incubation with 100 µg/ml proteinase K for additional 2 h at 50 °C. SYTOX Green (Invitrogen) at 2 µM was added to the cells before the analysis in a BD FACStar cell sorter.

3D structural analysis

All 3D graphical images from the yeast 80S ribosomal structure (PDB ID 3O58 and 3O2Z)⁵⁹ were generated using Pymol software (Schrödinger).

Supplementary Material

Refer to Web version on PubMed Central for supplementary material.

ACKNOWLEDGEMENTS

We thank J.R. Cussiol and M. Smolka (Cornell University) for the yeast deletion templates, support in yeast genetics and comments in the manuscript. We are grateful to G. Hsu and R. Schneider for technical support in polysome analysis, and V. Subramanian and A. Hochwagen in FACS analysis. We thank N. Brandt, D. Gresham (New York University), M. Hochstrasser (Yale University), M.A. Osley (University of New Mexico) and R. Ratan (Burke Medical Research Institute) for sharing yeast strains and HT22 cells. We thank J.R. Chapman for assistance with targeted mass spectrometry, and the PRIDE Team for assistance with mass spectrometry data deposition. We are indebted to D. Gresham, J. Davis, E. Miraldi, and T. Rock for feedback on the manuscript. This work was supported in part by US National Science Foundation EAGER grant MCB-1355462 (G.M.S., C.V.), in part by the Zegar Family Foundation Fund for Genomics Research at NYU (G.M.S., C.V.), and in part by US National Institutes of Health grant GM43601 (D.F.).

REFERENCES

1. Herrero E, Ros J, Belli G, Cabiscol E. Redox control and oxidative stress in yeast cells. *Biochim Biophys Acta*. 2008; 1780:1217–1235. [PubMed: 18178164]
2. Apel K, Hirt H. Reactive oxygen species: metabolism, oxidative stress, and signal transduction. *Annual review of plant biology*. 2004; 55:373–399.

3. Klaunig JE, Kamendulis LM. The role of oxidative stress in carcinogenesis. *Annual review of pharmacology and toxicology*. 2004; 44:239–267.
4. Droege W. Free radicals in the physiological control of cell function. *Physiol Rev*. 2002; 82:47–95. [PubMed: 11773609]
5. Finkel T, Holbrook NJ. Oxidants, oxidative stress and the biology of ageing. *Nature*. 2000; 408:239–247. [PubMed: 11089981]
6. Morano KA, Grant CM, Moye-Rowley WS. The response to heat shock and oxidative stress in *Saccharomyces cerevisiae*. *Genetics*. 2012; 190:1157–1195. [PubMed: 22209905]
7. Goldberg AL. Protein degradation and protection against misfolded or damaged proteins. *Nature*. 2003; 426:895–899. [PubMed: 14685250]
8. Glickman MH, Ciechanover A. The ubiquitin-proteasome proteolytic pathway: destruction for the sake of construction. *Physiol Rev*. 2002; 82:373–428. [PubMed: 11917093]
9. Reyes-Turcu FE, Ventii KH, Wilkinson KD. Regulation and cellular roles of ubiquitin-specific deubiquitinating enzymes. *Annu Rev Biochem*. 2009; 78:363–397. [PubMed: 19489724]
10. Komander D, Clague MJ, Urbe S. Breaking the chains: structure and function of the deubiquitinases. *Nat Rev Mol Cell Biol*. 2009; 10:550–563. [PubMed: 19626045]
11. Finley D, Ulrich HD, Sommer T, Kaiser P. The ubiquitin-proteasome system of *Saccharomyces cerevisiae*. *Genetics*. 2012; 192:319–360. [PubMed: 23028185]
12. Hershko A, Ciechanover A, Heller H, Haas AL, Rose IA. Proposed role of ATP in protein breakdown: conjugation of protein with multiple chains of the polypeptide of ATP-dependent proteolysis. *Proc Natl Acad Sci U S A*. 1980; 77:1783–1786. [PubMed: 6990414]
13. Spence J, Sadis S, Haas AL, Finley D. A ubiquitin mutant with specific defects in DNA repair and multiubiquitination. *Mol Cell Biol*. 1995; 15:1265–1273. [PubMed: 7862120]
14. Komander D. The emerging complexity of protein ubiquitination. *Biochem Soc Trans*. 2009; 37:937–953. [PubMed: 19754430]
15. Chen ZJ, Sun LJ. Nonproteolytic functions of ubiquitin in cell signaling. *Mol Cell*. 2009; 33:275–286. [PubMed: 19217402]
16. Xu P, et al. Quantitative proteomics reveals the function of unconventional ubiquitin chains in proteasomal degradation. *Cell*. 2009; 137:133–145. [PubMed: 19345192]
17. Matsumoto ML, et al. K11-linked polyubiquitination in cell cycle control revealed by a K11 linkage-specific antibody. *Mol Cell*. 2010; 39:477–484. [PubMed: 20655260]
18. Lauwers E, Jacob C, Andre B. K63-linked ubiquitin chains as a specific signal for protein sorting into the multivesicular body pathway. *J Cell Biol*. 2009; 185:493–502. [PubMed: 19398763]
19. MacDonald C, Buchkovich NJ, Stringer DK, Emr SD, Piper RC. Cargo ubiquitination is essential for multivesicular body intraluminal vesicle formation. *EMBO Rep*. 2012; 13:331–338. [PubMed: 22370727]
20. Hoege C, Pfander B, Moldovan GL, Pyrowolakis G, Jentsch S. RAD6-dependent DNA repair is linked to modification of PCNA by ubiquitin and SUMO. *Nature*. 2002; 419:135–141. [PubMed: 12226657]
21. Deng L, et al. Activation of the IkappaB kinase complex by TRAF6 requires a dimeric ubiquitin-conjugating enzyme complex and a unique polyubiquitin chain. *Cell*. 2000; 103:351–361. [PubMed: 11057907]
22. Zhou H, et al. Bcl10 activates the NF-kappaB pathway through ubiquitination of NEMO. *Nature*. 2004; 427:167–171. [PubMed: 14695475]
23. Dudek EJ, et al. Selectivity of the ubiquitin pathway for oxidatively modified proteins: relevance to protein precipitation diseases. *FASEB J*. 2005; 19:1707–1709. [PubMed: 16099947]
24. Medicherla B, Goldberg AL. Heat shock and oxygen radicals stimulate ubiquitin-dependent degradation mainly of newly synthesized proteins. *J Cell Biol*. 2008; 182:663–673. [PubMed: 18725537]
25. Shringarpure R, Grune T, Mehlhase J, Davies KJ. Ubiquitin conjugation is not required for the degradation of oxidized proteins by proteasome. *J Biol Chem*. 2003; 278:311–318. [PubMed: 12401807]

26. Pickering AM, et al. The immunoproteasome, the 20S proteasome and the PA28alpha/beta proteasome regulator are oxidative-stress-adaptive proteolytic complexes. *Biochem J.* 2010; 432:585–594. [PubMed: 20919990]

27. Peterson AC, Russell JD, Bailey DJ, Westphall MS, Coon JJ. Parallel reaction monitoring for high resolution and high mass accuracy quantitative, targeted proteomics. *Mol Cell Proteomics.* 2012; 11:1475–1488. [PubMed: 22865924]

28. Kirkpatrick DS, Denison C, Gygi SP. Weighing in on ubiquitin: the expanding role of mass-spectrometry-based proteomics. *Nat Cell Biol.* 2005; 7:750–757. [PubMed: 16056266]

29. Lee BH, et al. Enhancement of proteasome activity by a small-molecule inhibitor of USP14. *Nature.* 2010; 467:179–184. [PubMed: 20829789]

30. Giannattasio M, Lazzaro F, Plevani P, Muzi-Falconi M. The DNA damage checkpoint response requires histone H2B ubiquitination by Rad6-Bre1 and H3 methylation by Dot1. *J Biol Chem.* 2005; 280:9879–9886. [PubMed: 15632126]

31. Fleming AB, Kao CF, Hillyer C, Pikaart M, Osley MA. H2B ubiquitylation plays a role in nucleosome dynamics during transcription elongation. *Mol Cell.* 2008; 31:57–66. [PubMed: 18614047]

32. Wood A, et al. Bre1, an E3 ubiquitin ligase required for recruitment and substrate selection of Rad6 at a promoter. *Mol Cell.* 2003; 11:267–274. [PubMed: 12535539]

33. Hwang CS, Shemorry A, Auerbach D, Varshavsky A. The N-end rule pathway is mediated by a complex of the RING-type Ubr1 and HECT-type Ufd4 ubiquitin ligases. *Nat Cell Biol.* 2010; 12:1177–1185. [PubMed: 21076411]

34. Dohmen RJ, Madura K, Bartel B, Varshavsky A. The N-end rule is mediated by the UBC2(RAD6) ubiquitin-conjugating enzyme. *Proc Natl Acad Sci U S A.* 1991; 88:7351–7355. [PubMed: 1651502]

35. Lee JS, et al. Histone crosstalk between H2B monoubiquitination and H3 methylation mediated by COMPASS. *Cell.* 2007; 131:1084–1096. [PubMed: 18083099]

36. Song YH, Ahn SH. A Bre1-associated protein, large 1 (Lge1), promotes H2B ubiquitylation during the early stages of transcription elongation. *J Biol Chem.* 2010; 285:2361–2367. [PubMed: 19923226]

37. Wood A, Schneider J, Dover J, Johnston M, Shilatifard A. The Paf1 complex is essential for histone monoubiquitination by the Rad6-Bre1 complex, which signals for histone methylation by COMPASS and Dot1p. *J Biol Chem.* 2003; 278:34739–34742. [PubMed: 12876294]

38. Piro AS, Mayekar MK, Warner MH, Davis CP, Arndt KM. Small region of Rtf1 protein can substitute for complete Paf1 complex in facilitating global histone H2B ubiquitylation in yeast. *Proc Natl Acad Sci U S A.* 2012; 109:10837–10842. [PubMed: 22699496]

39. Tercero JA, Diffley JF. Regulation of DNA replication fork progression through damaged DNA by the Mec1/Rad53 checkpoint. *Nature.* 2001; 412:553–557. [PubMed: 11484057]

40. Spence J, et al. Cell cycle-regulated modification of the ribosome by a variant multiubiquitin chain. *Cell.* 2000; 102:67–76. [PubMed: 10929714]

41. Tan JM, et al. Lysine 63-linked ubiquitination promotes the formation and autophagic clearance of protein inclusions associated with neurodegenerative diseases. *Hum Mol Genet.* 2008; 17:431–439. [PubMed: 17981811]

42. Saeki Y, et al. Lysine 63-linked polyubiquitin chain may serve as a targeting signal for the 26S proteasome. *EMBO J.* 2009; 28:359–371. [PubMed: 19153599]

43. Grant CM. Regulation of translation by hydrogen peroxide. *Antioxid Redox Signal.* 2011; 15:191–203. [PubMed: 21126188]

44. Shenton D, et al. Global translational responses to oxidative stress impact upon multiple levels of protein synthesis. *J Biol Chem.* 2006; 281:29011–29021. [PubMed: 16849329]

45. Lee JG, Baek K, Soetandyo N, Ye Y. Reversible inactivation of deubiquitinases by reactive oxygen species in vitro and in cells. *Nature communications.* 2013; 4:1568.

46. Cotto-Rios XM, Békes M, Chapman J, Ueberheide B, Huang TT. Deubiquitinases as a signaling target of oxidative stress. *Cell reports.* 2012; 2:1475–1484. [PubMed: 23219552]

47. Kee Y, Munoz W, Lyon N, Huibregtse JM. The deubiquitinating enzyme Ubp2 modulates Rsp5-dependent Lys63-linked polyubiquitin conjugates in *Saccharomyces cerevisiae*. *J Biol Chem*. 2006; 281:36724–36731. [PubMed: 17028178]

48. Komander D, et al. Molecular discrimination of structurally equivalent Lys 63-linked and linear polyubiquitin chains. *EMBO Rep*. 2009; 10:466–473. [PubMed: 19373254]

49. Netto LE, et al. Reactive cysteine in proteins: protein folding, antioxidant defense, redox signaling and more. *Comp Biochem Physiol C Toxicol Pharmacol*. 2007; 146:180–193. [PubMed: 17045551]

50. Ritorto MS, et al. Screening of DUB activity and specificity by MALDI-TOF mass spectrometry. *Nature communications*. 2014; 5:4763.

51. Tomanov K, Luschnig C, Bachmair A. Ubiquitin Lys 63 chains - second-most abundant, but poorly understood in plants. *Frontiers in plant science*. 2014; 5:15. [PubMed: 24550925]

52. Peng J, et al. A proteomics approach to understanding protein ubiquitination. *Nat Biotechnol*. 2003; 21:921–926. [PubMed: 12872131]

53. Herman PK. Stationary phase in yeast. *Curr Opin Microbiol*. 2002; 5:602–607. [PubMed: 12457705]

54. El-Sharoud WM, Niven GW. The influence of ribosome modulation factor on the survival of stationary-phase *Escherichia coli* during acid stress. *Microbiology*. 2007; 153:247–253. [PubMed: 17185553]

55. Yoshida H, Ueta M, Maki Y, Sakai A, Wada A. Activities of *Escherichia coli* ribosomes in IF3 and RMF change to prepare 100S ribosome formation on entering the stationary growth phase. *Genes to cells : devoted to molecular & cellular mechanisms*. 2009; 14:271–280. [PubMed: 19170772]

56. Kim W, et al. Systematic and quantitative assessment of the ubiquitin-modified proteome. *Mol Cell*. 2011; 44:325–340. [PubMed: 21906983]

57. Gerashchenko MV, Lobanov AV, Gladyshev VN. Genome-wide ribosome profiling reveals complex translational regulation in response to oxidative stress. *Proc Natl Acad Sci U S A*. 2012; 109:17394–17399. [PubMed: 23045643]

58. Vogel C, Silva GM, Marcotte EM. Protein expression regulation under oxidative stress. *Mol Cell Proteomics*. 2011; 10:M111.009217. [PubMed: 21933953]

59. Ben-Shem A, Jenner L, Yusupova G, Yusupov M. Crystal structure of the eukaryotic ribosome. *Science*. 2010; 330:1203–1209. [PubMed: 21109664]

60. Liu C, Apodaca J, Davis LE, Rao H. Proteasome inhibition in wild-type yeast *Saccharomyces cerevisiae* cells. *Biotechniques*. 2007; 42:158, 160, 162. [PubMed: 17373478]

61. Ramirez-Valle F, Braunstein S, Zavadil J, Formenti SC, Schneider RJ. eIF4GI links nutrient sensing by mTOR to cell proliferation and inhibition of autophagy. *J Cell Biol*. 2008; 181:293–307. [PubMed: 18426977]

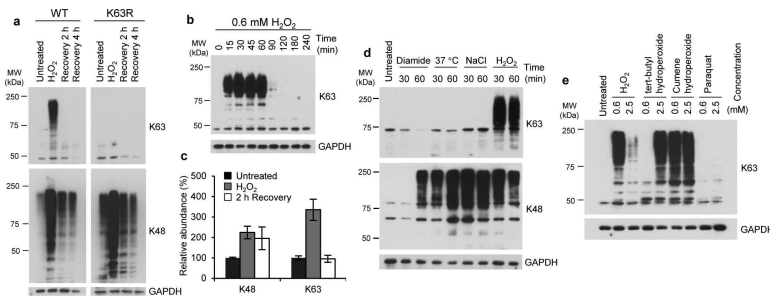


Figure 1. K63 polyubiquitin transiently accumulates in response to H₂O₂

a, Anti-K63- and K48- specific ubiquitin western blot of lysates from WT and K63R cells upon treatment with, and subsequent recovery from, 0.6 mM H₂O₂. **b**, Anti-K63 ubiquitin western blot of lysate from WT cells treated with H₂O₂ for different amounts of time. **c**, Histogram showing dynamics of K63 and K48 ubiquitin linkages measured by quantitative targeted mass spectrometry. Plot shows mean of two biological replicates with two technical replicates each, and error bars indicate the range of values across the replicates. **d**, Anti-K63 and anti-K48 ubiquitin western blot of lysate from WT cells subjected to indicated compounds and heat-shock for designated times. **e**, Anti-K63 ubiquitin western blot of lysate from WT cells treated with the indicated oxidizing agents for 30 min. Anti-GAPDH was used as loading control. WT, wild-type SUB280 yeast strain. K63R, ubiquitin K63R mutant SUB413 yeast strain. MW, molecular weight.

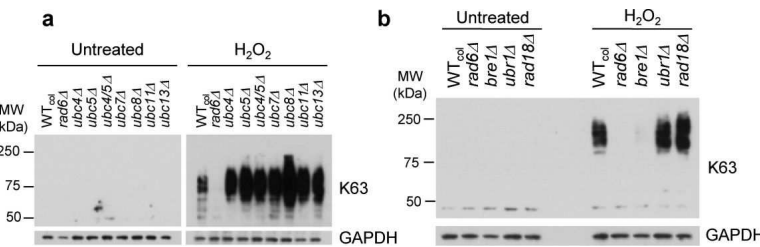


Figure 2. Rad6-Bre1 conjugate K63 polyubiquitination in response to H_2O_2

(a,b) Anti-K63 ubiquitin western blot of lysates from (a) E2 and (b) Rad6-interacting-E3 deleted cells in the presence and absence of 0.6 mM H_2O_2 . Anti-GAPDH was used as loading control. WT_{col}, wild-type cells S288c used with the deletion collection. MW, molecular weight.

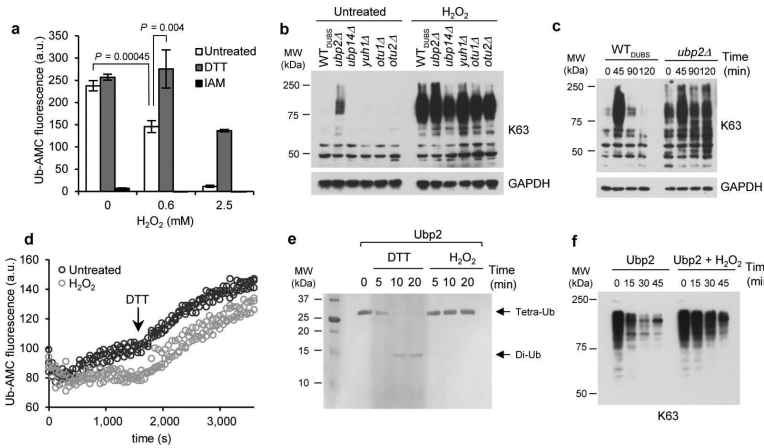


Figure 3. Ubp2 is reversibly inhibited by H₂O₂

a, Histogram with activity of intracellular DUBs from WT cells treated with the indicated concentrations of H₂O₂. Activity was measured after incubation of cellular lysate with the Ub-AMC fluorogenic substrate. Error bar, s.d. (*P* values were calculated using paired, one-tailed Student's *t*-test, *n* = 3 independent cell growth). **(b,c)** Anti-K63 ubiquitin western blot of lysates from **(b)** DUB deleted cells in the presence or absence of H₂O₂ and **(c)** WT and *ubp2Δ* after H₂O₂ treatment for different amount of times. **d**, Scatter plot with activity of native purified TAP-tagged Ubp2 (black) and 0.5 mM H₂O₂-treated Ubp2 (grey), measured after incubation with Ub-AMC fluorogenic substrate for the indicated times. Arrow indicates addition of 10 mM DTT. **e**, SDS-PAGE gel of 1 μ g K63 tetra-ubiquitin chains after incubation for the indicated times with purified Ubp2 treated with 10 mM DTT or 0.5 mM H₂O₂. **f**, Anti-K63 ubiquitin blot of lysate from cells treated with H₂O₂ after incubation with native or H₂O₂-treated TAP-tagged Ubp2. Samples were incubated without DTT to prevent activation of intracellular DUBs. Anti-GAPDH was used as loading control. WT_{DUBs}, wild-type yeast strain SUB62. a.u., fluorescence arbitrary units. MW, molecular weight.

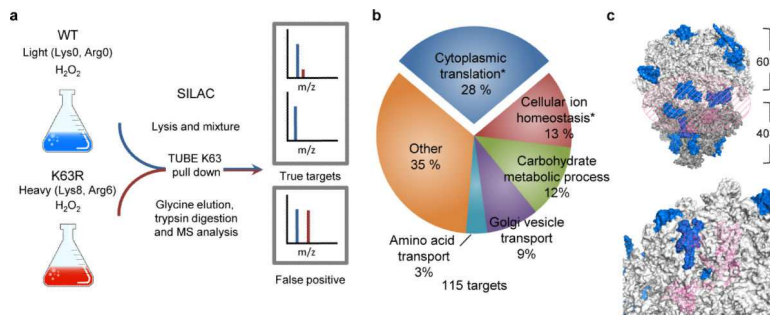


Figure 4. Ribosomal proteins are a main target of K63 polyubiquitination under H_2O_2 stress

a, Scheme describing the SILAC LC-MS/MS approach used to identify and quantify K63 conjugates by high-resolution mass spectrometry. **b**, Chart showing gene ontology (GO) annotation for K63 ubiquitinated targets using DAVID functional annotation tool. (*) GO enrichment significant at FDR < 0.005 %. **c**, Surface 3D structure shows mapping of ribosomal proteins modified by K63 ubiquitination (blue) onto the 80S ribosome particle. The 60S large unit (PDB ID 3O58)⁵⁹ is represented in light grey and the 40S small unit (PDB ID 3O2Z)⁵⁹ is in dark grey. In pink, we highlight proteins in the mRNA-tRNA interaction sites (top panel) and in the ribosome exit tunnel (bottom panel). WT, wild-type SILAC GMS280 yeast strain. K63R, ubiquitin K63R mutant SILAC GMS413 yeast strain.

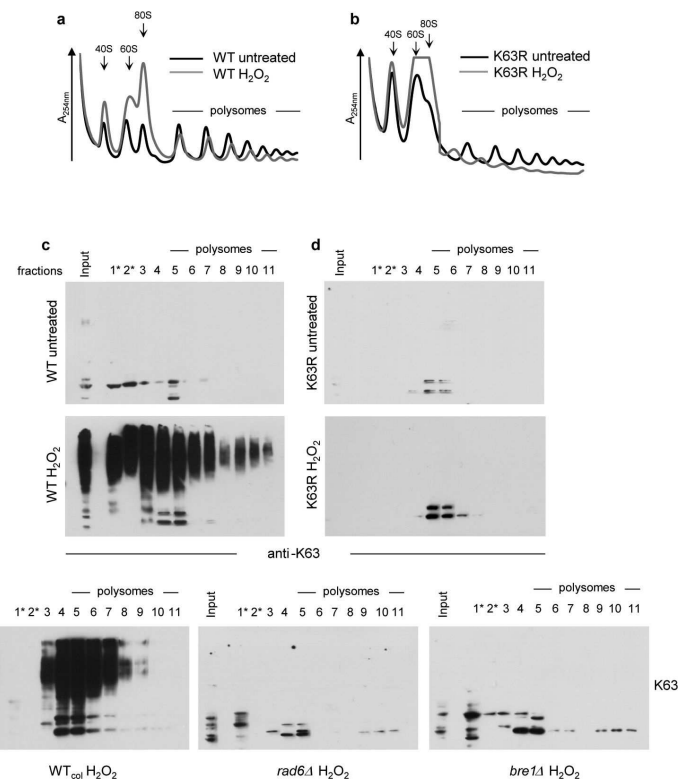


Figure 5. K63 ubiquitin modifies proteins in monosome and polysome fractions

(a,b), Sucrose sedimentation profiles of polysomes from the (a) WT and (b) K63R mutant cells extracted using a physiological MgCl₂ concentration (3 mM). (c–e) Anti-K63 ubiquitin western blot from stabilized polysomes extracted using 30 mM MgCl₂ from (c) WT and (d) K63R mutant cells or (e) WT_{col}, rad6Δ and bre1Δ cells. Ponceau-S loading control is shown in Supplementary Fig. 5. (*) Half of the sample volume was loaded for better visualization. WT, wild-type SUB280 yeast strain, K63R, ubiquitin K63R mutant SUB413 yeast strain. WT_{col}, wild-type cells S288c used with the deletion collection. MW, molecular weight.

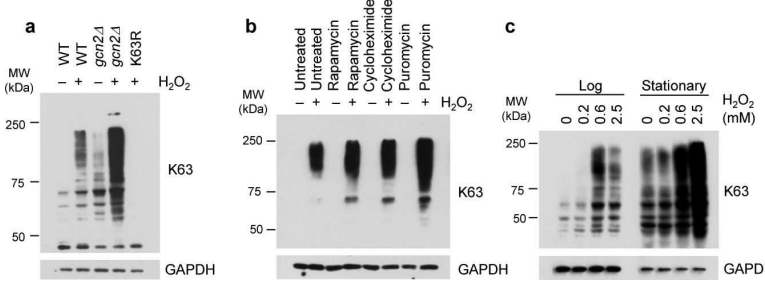


Figure 6. K63 ubiquitination is linked to active translation

(a–c) Anti-K63 ubiquitin western blot of lysates from (a) WT, *gcn2Δ* and K63R mutant cells, (b) WT cells treated for 30 min with designated translation inhibitors prior to H₂O₂ treatment and (c) WT cells grown into Log phase OD₆₀₀ = 0.4 or after 24 h in culture starting from OD₆₀₀ = 0.2 (Stationary), in the presence (+) or absence (−) of the indicated compounds. Anti-GAPDH was used as loading control. WT, wild-type SUB280 yeast strain. K63R, ubiquitin K63R mutant SUB413 yeast strain. MW, molecular weight.

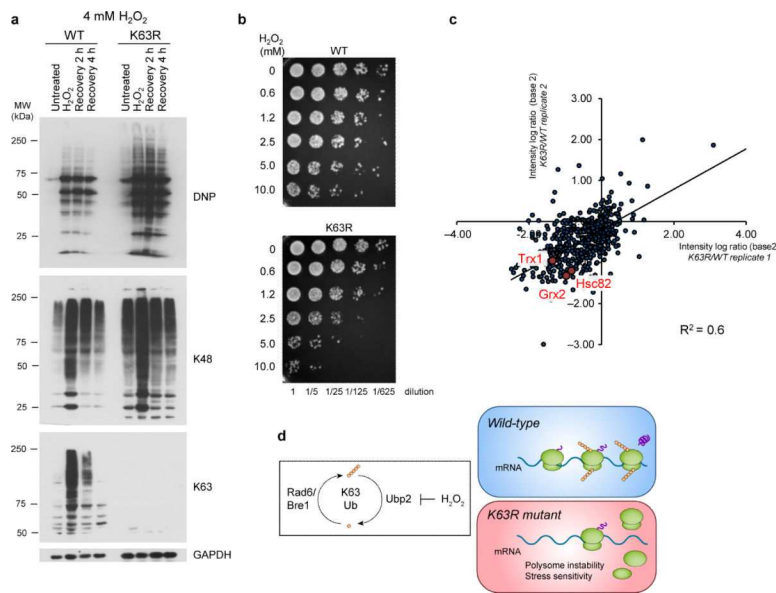


Figure 7. Lack of K63 ubiquitin impacts cellular resistance to oxidative stress

a, Anti-DNP (oxidation), anti-K63 and anti-K48 ubiquitin western blots of cell lysate from WT and K63R mutant cells upon treatment with, and subsequent recovery from, 4 mM H₂O₂. Anti-GAPDH was used as loading control. **b**, Serial dilution assays from WT and K63R mutant cells treated with different amounts of H₂O₂. After stress induction cells were spotted onto YPD plates without H₂O₂. **c**, Correlation plot showing log base 2 SILAC ratio K63R/WT for the mass spectrometry data from cell lysate replicates. We highlighted individual examples of stress-related proteins with decreased expression to less than 25 % in the K63R mutant compared to the levels found in the WT. Pearson correlation coefficient is 0.60. **d**, Model of the role of K63 polyubiquitination during the translation cycle in response to H₂O₂. WT, wild-type SUB280 yeast strain. K63R, ubiquitin K63R mutant SUB413 yeast strain. MW, molecular weight.